Amplitude Variation with Ray Parameter Analysis Using the Reflection Impedance Concept

Lúcio Tunes Santos and Martin Tygel, DMA – IMECC – UNICAMP, Brazil

Abstract

The Common Relection Surface method provides semblance and attributes panels, which gives information about the ray-parameter at the reflection point at possible interfaces in the elastic model. The reflection impedance function, gives an approximation for the reflection coefficient which is suitable for inversion purposes. Combining both procedures, we have a practical amplitude versus ray-parameter analysis which is suitable for inversion of rock-propertie parameters.

Introduction

The *Normal Moveout (NMO)* considers, in its two-dimensional version, a Common Midpoint (CMP) gather of sources and receivers along a horizontal seismic line. The reflection traveltimes along offset rays not far from the Zero-Offset (ZO) ray at the CMP are approximated by the one-parameter hyperbolic formula (Dix, 1955)

$$T(h) = \sqrt{T_0^2 + C\,h^2}\ . \qquad (1)$$

In the above equation, T is the traveltime from the source to the reflector and back to the receiver, T_0 is the ZO traveltime at the CMP, h is the half-offset between shot and receiver. Finally,

$$C = \frac{4}{V_{NMO}^2}\ , \qquad (2)$$

where V_{NMO} is the NMO-velocity, is the single parameter that is to be inverted from the CMP data. Note that the square of the NMO equation (1) can readily be seen as a second-order Taylor expansion with respect to half-offset.

As shown in Castagna & Backus (1993) the ray parameter for the reflection ray in the CMP gather can be approximated by

$$p = \frac{1}{2}\frac{d}{dh}T(h) = \frac{C}{2\,\sqrt{C + T_0^2/h^2}}\ . \qquad (3)$$

Applying a coherence (semblance) analysis to the CMP data it is possible to fit an hyperbola to the traveltimes and then, extract parameter C, or V_{NMO}. Using formula (3), the ray parameter is also extracted.

The following step is to perform an inversion based on the amplitudes versus the corresponding ray parameters of the CMP rays. In other words, an Amplitude Variation with p (AVP) analysis. Figure 1 ilustrates the described process for a synthetic model.

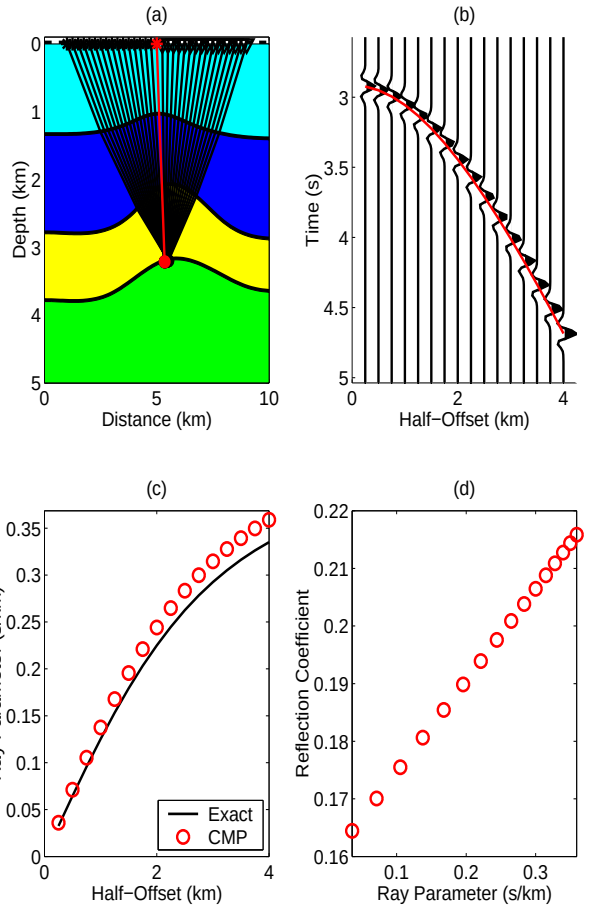

Figure 1: Example of an AVP analysis: (a) Synthetic model with CMP rays; (b) CMP section with fitted hyperbola; (c) Exact and extracted ray parameter; (d) Amplitude variation with ray parameter.

The Commom Reflection Surface Method

After Hubral (1983), the concepts of the Normal (N) and Normal-Incident-Point (NIP) waves were incorporated in the Taylor formulation of the reflection moveouts in the vicinity of the ZO ray. The 2D ZO Common Reflection Surface (CRS) method uses the hyperbolic normal moveout (see, e.g., Müller et al., 1998)

$$T(x,h) = \sqrt{[T_0 + A\,x]^2 + B\,x^2 + C\,h^2}\ , \qquad (4)$$

where x and h denote the midpoint (relative to the central point) and half-offset coordinates of the source and receiver pair, and T_0 is the ZO traveltime at the central point.

The parameters A, B and C are related to physical quantities referred to as the CRS parameters,

$$A = \frac{2\sin\phi}{v_0},\ B = \frac{2T_0\cos^2\phi}{v_0}K_N,\ C = \frac{2T_0\cos^2\phi}{v_0}K_{NIP}, \tag{5}$$

where ϕ is the emergence angle of the ZO ray with respect to the surface normal, and K_N and K_{NIP} are the curvatures of the N- and NIP-waves, respectively. All these quantities evaluated at the central point. Finally, v_0 is the medium velocity at the central point. Observe that formula (4) reduces to the normal-moveout (1) in the case of a CMP gather, i.e., $x = 0$. Moreover, the relation between V_{NMO} and the CRS parameters is clear,

$$V_{NMO}^2 = \frac{4}{C} = \frac{2\ v_0}{T_0\ \cos^2\phi\ K_{NIP}}\ . \tag{6}$$

The CRS method can then be also used to perform an amplitude versus ray-parameter analysis, in the same way as it is done in the CMP method. The advantage of the CRS strategy is that the semblance analysis is applied for a grid of possible values for the central point and the ZO traveltime, using all gathers and not only the CMP ones.

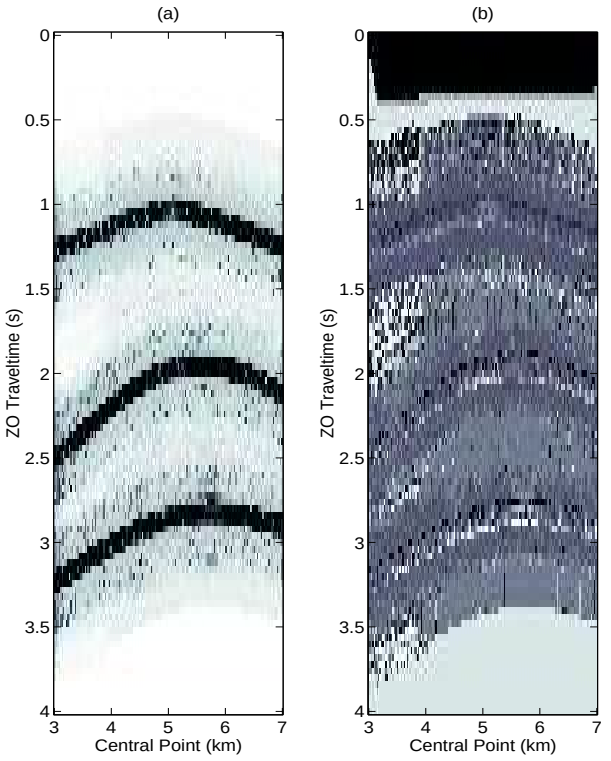

Figure 2: (a) Semblance panel obtained from the CRS method applied to the same synthetic model in Figure 1(a); (b) Respective C-parameter panel.

After the coherence step, it is possible to select regions with high values of the semblance function and then extract the ray parameter, using formula (3), from the respectives values of the parameter C. In Figure 2 we show the semblance panel obtained from the CRS method applied to the same synthetic model in Figure 1(a), together with the respective C-parameter panel.

Reflection Impedance

As introduced in Connolly (1999) and discussed in Santos & Tygel (2004), it is possible to define an impedance function (I), for which the P-P reflection coefficient can be given, at least approximately, by

$$R_{PP} = \frac{I(\rho_2,\alpha_2,\beta_2,p) - I(\rho_1,\alpha_1,\beta_1,p)}{I(\rho_2,\alpha_2,\beta_2,p) + I(\rho_1,\alpha_1,\beta_1,p)}\ , \tag{7}$$

where ρ_j, α_j, β_j denote the density and P- and S-wave velocities, respectively, at the incident side $(j = 1)$ and at the opposite side $(j = 2)$ of the reflecting interface. Moreover, p is the ray parameter given by $p = \sin\theta/\alpha_1$ and θ is the incidence angle.

Under the assumption of a Gardner's type relationship between ρ and β,

$$\rho = b\ \beta^{\gamma}\ , \tag{8}$$

where b is some constant of proportionality and γ is a constant, Santos et al. (2002) introduced the reflection impedance function, given by

$$I = \frac{\rho\ \alpha}{\sqrt{1-\alpha^2p^2}}\ \exp\{-2[2+\gamma]\beta^2p^2\}\ . \tag{9}$$

Connoly (1999) introduced a different expression, named the elastic impedance function, under the assumption of a constant $K = \beta^2/\alpha^2$ ratio,

$$I = \rho^{1\ -\ 4K\sin^2\theta}\ \alpha^{\sec^2\theta}\ \beta^{-8K\sin^2\theta}\ . \tag{10}$$

In Figure 3 we compare the approximation formula (7) for a representative elastic model. Both approximations using elastic and reflection impedance functions are plotted, together with the linear approximation of Aki & Richards (1980). Observe the accuracy of the reflection impedance function, even for critical values of the incidence angle.

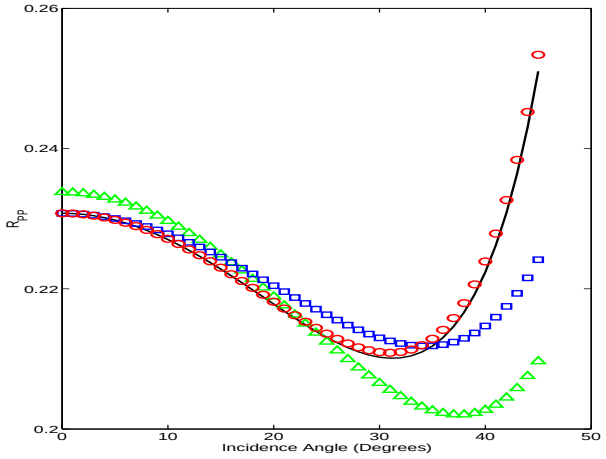

Figure 3: Approximations for R_{PP}: Exact (—), Linear (Δ), Elastic Impedance ($\square$), and Reflection Impedance ($\circ$).

AVP Inversion

From equations (7) and (9) we can write

$$R_{PP}(p) = \frac{J(p)-1}{J(p)+1}\ , \tag{11}$$

where

$$J(p) = \frac{I(\rho_2, \alpha_2, \beta_2, p)}{I(\rho_1, \alpha_1, \beta_1, p)} = \Lambda_3 \sqrt{\frac{1 - \Lambda_1^2\, p^2}{1 - \Lambda_2^2\, p^2}}\ \exp\{\Lambda_4\, p^2\}\ , \tag{12}$$

with

$$\Lambda_1 = \alpha_1,\ \Lambda_2 = \alpha_2,\ \Lambda_3 = \frac{\rho_2\ \alpha_2}{\rho_1\ \alpha_1}, \tag{13}$$

and

$$\Lambda_4 = -2[2 + \gamma](\beta_2^2 - \beta_1^2)\ . \tag{14}$$

Given a set of ray-parameters $\{p_n\}$ and the respectives reflection coefficients,$\{R_n\}$, we can apply a least-squares procedure to invert for the parameters Λ_i. The optimization problem to be solved is then

$$\min_{\Lambda_i} \sum_{n=1}^{N} \left[R_n - \frac{J(p_n) - 1}{J(p_n) + 1} \right]^2\ . \tag{15}$$

After the optimal solution is found, we compute the inverted ratios for P-wave velocity and density,

$$\frac{\alpha_2}{\alpha_1} = \frac{\Lambda_2}{\Lambda_1}, \quad \text{and} \quad \frac{\rho_2}{\rho_1} = \Lambda_3\ \frac{\Lambda_1}{\Lambda_2}\ . \tag{16}$$

To extract the ratio for the S-wave velocity, additional information about the data is needed. For example, from a well-log analysis, if we estimate the value of the contant γ in equation (8), then

$$\frac{\beta_2}{\beta_1} = \left(\frac{\rho_2}{\rho_1}\right)^{1/\gamma}\ . \tag{17}$$

Numerical Experiments

In order to analyse the accuracy of the AVP analysis presented above, we consider the two-layer model depicted in Figure 4. For each interface, the values for the S-wave velocities are the values of the P-wave velocity divided by $\sqrt{2}$ and $\sqrt{3}$, above and below the interface, respectively; for density, we take 1.2 g/cm^3 and 1.5 g/cm^3, above and below the interface, respectively. The CRS method was applied for central points $x_0 \in [3, 7]$ km and ZO traveltimes $T_0 \in [0, 4]$.

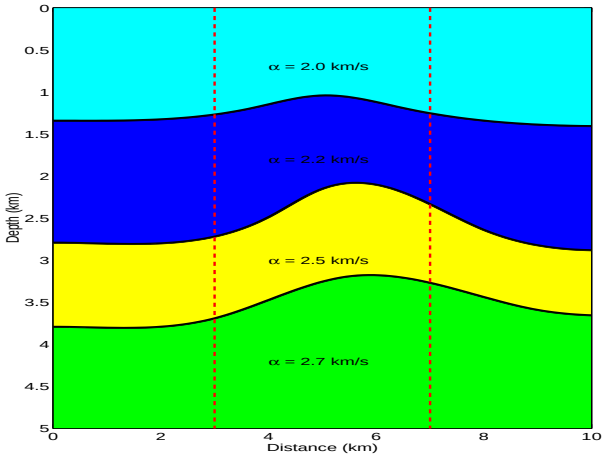

Figure 4: Synthetic model for the numerical experiments.

For each of the three interfaces, we select a box region with high values of the semblance funtion, and apply the inversion procedure for each x_0 in the box twice: using the correct values for the P-P reflection coefficient and adding 10% noise. For the constant γ, from equation (17) we use the averaged value

$$\frac{1}{\gamma} = \frac{1}{3} \frac{\ln \sum_{j=1}^{3} [\beta_{j+1}/\beta_j]}{\ln(1.5/1.2)} = -0.4795\ . \tag{18}$$

Figures 5–7 show the results. Please observe that since the layers are homogeneous, each parameter ratio is constant along the x_0-axis for each reflector.

Conclusions

We have discussed the problem of inversion for ratios of elastic parameters, using a combination of the CRS method and an impedance-type approximation for the P-P reflection coefficient. The CRS method provides semblance and attributes panels, which gives information about the ray-parameter at the reflection point at possible interfaces in the elastic model. The reflection impedance function gives an approximation for the reflection coefficient which is suitable for inversion purposes. The result is a practical amplitude variation with ray-parameter analysis.

Our simple, but typical, numerical experiments have shown that the process has the potential to be applied for real data.

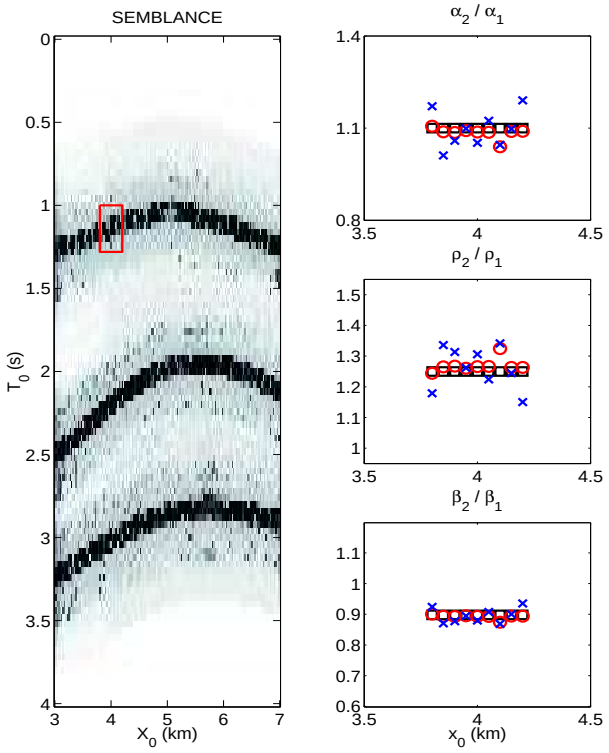

Figure 5: Parameter ratios for a window in the first reflector: Modeled (□), inverted without noise (○), and inverted with 10% noise (×).

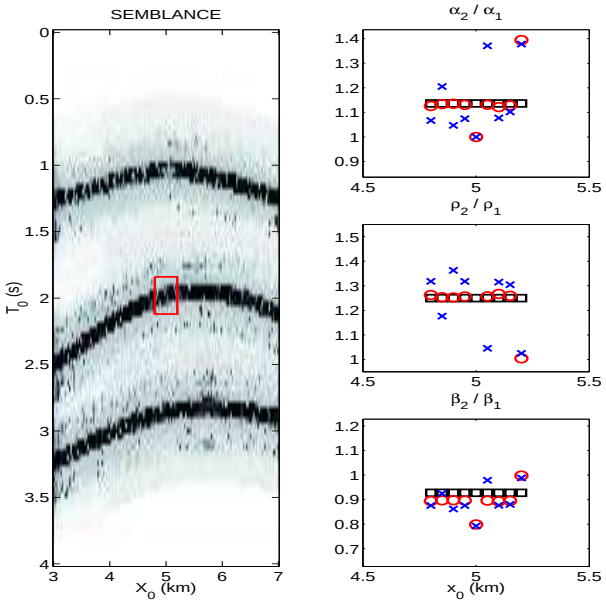

Figure 6: Parameter ratios for a window in the second reflector: Modeled (□), inverted without noise (○), and inverted with 10% noise (×).

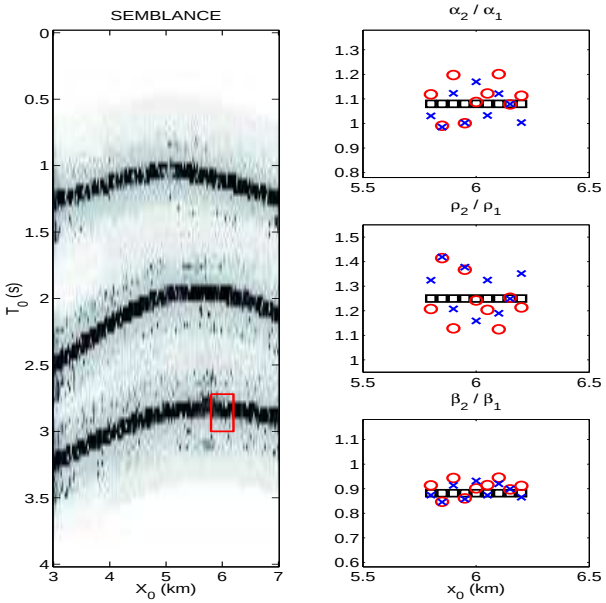

Figure 7: Parameter ratios for a window in the third reflector: Modeled (□), inverted without noise (○), and inverted with 10% noise (×).

Acknowledgements

We thank CNPq (Grants 307165/2003-5 & 301733/2004-0) and FAPESP (Grant 01/01068-0), Brazil, and the sponsors of the WIT – Wave Inversion Technology Consortium, Germany.

References

Aki, K.I., and P.G. Richards, 1980, Quantitative Seismology, W.H. Freeman and Co.

Castagna, J.P., and M.M. Backus, eds., 1993, Offset-Dependent reflectivity – Theory and Practice of AVO Analysis, SEG.

Connolly, P., 1999, Elastic Impedance, The Leading Edge, 18, 438–452.

Dix, C.H., 1955, Seismic Velocities from Surface Measurements, Geophysics, 20, 68–86.

Hubral, P., 1983, Computing True Amplitude Reflections in a Laterally Inhomogeneous Earth, Geophysics, 48, 1051–1062.

Müller, T., R. Jäger, and G. Höcht, 1998, Common Reflection Surface Stacking Method - Imaging with an Unknown Velocity Model, 68th EAGE Conference & Exhibition, Expanded Abstracts, 1764–1767.

Santos, L.T., M. Tygel, and A.C.B. Ramos, 2002, Reflection Impedance, 64th European Association of Geoscientists & Engineers Conference,P-182.

Santos, L.T., and M. Tygel, 2004, Impedance-Type Approximations of the P-P Elastic Reflection Coefficient: Modeling and AVO Inversion, Geophysics, 69, 592–598.